**Crustal conditions favoring convective downward migration of fractures in deep hydrothermal systems**

Sæunn Halldórsdóttir[1], Inga Berre[1], Eirik Keilegavlen[1], and Gudni Axelsson [2]

[1]University of Bergen, Center for Modeling of Subsurface Dynamics, Department of Mathematics, University of Bergen, Allégaten 41, 5007 Bergen.

[2]ÍSOR, Icelandic GeoSurvey, Urdarhvarf 8, 203 Kópavogur.

## Contents of this file

## Introduction

This document provides the governing equations that underlies the simulation model used for the paper 'Crustal conditions favoring convective downward migration of fractures in deep hydrothermal systems', referred to below as 'the paper'. It is divided into the following subsections:

- Thermo-poroelasticity, energy and mass balance in the rock matrix
- Fracture deformation and energy and mass balance in the fracture
- Tensile stress and fracture propagation
- Notes on the numerical implementation

**Text S1.**

For the modelling of hydrothermal reservoirs, we use a mathematical model based on a discrete fracture matrix method, that describes energy transport and fluid flow in a fractured deformable porous medium. The medium is 3D, consisting of rock matrix and

embedded fractures modelled as 2D planes. Single phase fluid is assumed, fully saturating the reservoir rock. Furthermore, local thermal equilibrium between the fluid and the solid is assumed. Effective coefficients for the fluid saturated rock matrix are estimated based on the fluid and rock coefficients and the porosity, $\phi$, according to:

$$(\text{coeff.})_e = \phi(\text{coeff.})_f + (1 - \phi)(\text{coeff.})_s. \tag{1}$$

We impose a balance of momentum, mass and energy in the rock matrix and balance of mass and energy in the fractures. The conservation equations described in this section are complemented by appropriate boundary conditions on the domain boundary (both matrix and fracture) described in section 4 of the paper.

**Thermo-poroelasticity, energy and mass balance in the rock matrix**

For quasi-static conditions, the linear momentum balance equation for an elementary volume in the rock matrix is given as

$$\nabla \cdot \boldsymbol{\sigma} = -\mathbf{F}, \tag{2}$$

with $\mathbf{F}$ being the body force per unit volume, and the total stress $\boldsymbol{\sigma}$ being composed of thermal, hydraulic and mechanical (THM) terms. By assuming linearity and using the convention that tensile stresses are positive, the stress-strain relationship for thermo-poroelasticity, resulting from perturbations from an initial temperature $T_0$ can be written

$$\boldsymbol{\sigma} = \text{D}:(\nabla\mathbf{u} + \nabla\mathbf{u}^\text{T})/2 - \alpha p\mathbf{I} - \beta_s B_s(T - T_0)\mathbf{I}, \tag{3}$$

where D is the drained stiffness matrix and the strain is related to the displacement vector of the rock, $\mathbf{u}$ by the symmetric gradient $(\nabla\mathbf{u} + \nabla\mathbf{u}^\text{T})/2$. Furthermore, $\alpha$ is the Biot coefficient, $p$ is fluid the pressure, $\mathbf{I}$ is the identity matrix, $\beta_s$ and $B_s$ are the volumetric thermal expansion and the bulk modulus of the rock, respectively, and ':' denotes the double dot product. Finally, we assume an isotropic medium and use $\text{D}:(\nabla\mathbf{u} + \nabla\mathbf{u}^\text{T})/2 = \lambda\,\text{tr}(\nabla\mathbf{u}) + \mu(\nabla\mathbf{u} + \nabla\mathbf{u}^\text{T})$, where $\mu$ is the shear modulus of the rock, and $\lambda$ the Lame coefficient. Using that $\lambda = B_s - 2\mu/3$, the momentum balance for thermo-poroelasticity becomes

$$\nabla \cdot \left[ (B_s - \tfrac{2}{3}\mu)\,\text{tr}(\nabla\mathbf{u})\mathbf{I} + \mu(\nabla\mathbf{u} + \nabla\mathbf{u}^\text{T}) - \beta_s B_s(T - T_0)\mathbf{I} - \alpha p\mathbf{I} \right] = -\mathbf{F}. \tag{4}$$

The fluid is assumed to be pure water and is modelled as slightly compressible

$$\rho_f = \rho_0 \exp\left[ \frac{1}{B_f}(p - p_0) - \beta_f(T - T_0) \right], \tag{5}$$

with $\beta_f$ and $B_f$, the thermal expansion and the bulk modulus of the fluid, respectively.

The Darcy velocity of the fluid within the rock is given by

$$\mathbf{v} = -\frac{k}{\eta}(\nabla p - \rho_f \mathbf{g}). \tag{6}$$

Here $k$ is the matrix permeability, $\eta$ is the fluid dynamic viscosity, and $\mathbf{g}$ the gravity vector.

To complete the thermo-poromechanics descriptions of the reservoir matrix balance of mass and energy is imposed. The mass balance equation is given by

$$\left( \frac{\phi}{B_f} + \frac{\alpha - \phi}{B_s} \right)\frac{\partial p}{\partial t} + \alpha\frac{\partial}{\partial t}(\nabla \cdot \mathbf{u}) - \beta_e\frac{\partial T}{\partial t} + \nabla \cdot \mathbf{v} = Q_p, \tag{7}$$

while the energy balance is governed by

$$\rho_e c_e \frac{\partial T}{\partial t} + \beta_s K_s T_0 \frac{\partial}{\partial t} (\nabla \cdot \mathbf{u}) + \nabla \cdot \left[ \rho_f c_f T \mathbf{v} - \kappa_e \nabla T \right] = Q_{\mathrm{T}}. \tag{8}$$

Heat and volumetric sources and sinks are represented by $Q_T$ and $Q_p$ respectively. The effective thermal expansion and conductivity tensors of the rock matrix are given by $\beta_e$ and $\kappa_e$, respectively, the effective density and specific heat by $\rho_e$ and $c_e$, respectively, and the specific heat of the fluid is given by $c_f$. Based on the assumption that the fluid is all in liquid phase, a low enthalpy description is used, that is, the internal energy of the fluid takes the same form as the internal energy of the rock. This results in a simplification in the energy equation, with, $\rho_e c_e$, being the effective heat capacity of the rock matrix.

The primary variables in the rock matrix are the temperature $T$, the pressure $p$ and the displacement $\mathbf{u}$.

**Fracture deformation and energy and mass balance in the fracture**

Dimension reduction for the mass and energy equations is necessary to derive the flow of mass and energy in the fluid-filled fractures. The dimension reduction is detailed in Stefansson et al., (2021a) and Keilegavlen et al. (2021a). For the mechanical forces on the fracture, we consider balance between the fracture contact traction force, $\lambda_F$, and fracture fluid pressure, $p_F$, and the higher-dimensional THM traction on the opposing fracture walls (fracture-matrix interfaces):

$$\begin{aligned} \lambda_F - p_F \mathbf{I} \cdot \mathbf{n}_M^+ &= \ \ \boldsymbol{\sigma}_M \cdot \mathbf{n}_M^+, \\ \lambda_F - p_F \mathbf{I} \cdot \mathbf{n}_M^+ &= -\boldsymbol{\sigma}_M \cdot \mathbf{n}_M^-. \end{aligned} \tag{9}$$

Here, $\boldsymbol{\sigma}_M$ denotes the matrix thermo-poroelastic stress tensor, and $\mathbf{n}_M^{\pm}$ are the matrix outward normal vectors on each side of the fracture. The two sides of the fracture are denoted by "+" and "-", respectively. The normal to the fracture is chosen to be equal to the matrix normal on the (+) side. Consequently, the primary variables in the fracture are the temperature $T$, the pressure $p$, the displacement $\mathbf{u}$ and the contact traction $\lambda_F$.

The fracture aperture of a dimensionally reduced fracture will be affected by fluid pressure as well as thermo-poromechanical forces in the matrix. It is given by

$$a = a_0 + [\![\mathbf{u}]\!]_{\mathrm{n}}, \tag{10}$$

with $a_0$ denoting the residual hydraulic aperture in the undeformed state, and $[\![\mathbf{u}]\!]_{\mathrm{n}}$ the normal component of a displacement-jump over the fracture, defined as

$$[\![\mathbf{u}]\!] = \mathbf{u}^+ - \mathbf{u}^-, \tag{11}$$

i.e., the difference in the displacement computed on the fracture walls on each side of the fracture (Figure 1b). A vector $\mathbf{b}_F$ can be decomposed into $b_n = \mathbf{b}_F \cdot \mathbf{n}_M^+$ and $\mathbf{b}_\tau = \mathbf{b}_F - b_n \mathbf{n}_M^+$, that is the normal and tangential components relative to the fracture.

The dilation of the fracture associated with a tangential (sharing) displacement $[\![\mathbf{u}]\!]_\tau$ due to the rough fracture surfaces is defined by a gap function (Stefansson, et al., 2021a):

$$g = \tan(\Psi) \, ||[\![\mathbf{u}]\!]_\tau||, \tag{12}$$

with $\Psi$ as the dilation angle described by (Barton, 1976). Hence, $g$, is the normal distance between the fracture walls when in mechanical contact. The relative motion between the fracture walls is described by a nonpenetration condition which constrains the fracture deformation in the normal direction:

$$\begin{aligned} [\![\mathbf{u}]\!]_{\mathrm{n}} - g &\geq 0, \\ \lambda_n([\![\mathbf{u}]\!]_{\mathrm{n}} - g) &= 0, \\ \lambda_n &\leq 0. \end{aligned} \tag{13}$$

It follows that the normal contact force, $\lambda_n$, is zero when a fracture is mechanically open and there is no mechanical contact across the fracture. Finally, a Coulomb friction law that governs sliding of the fracture is given:

$$||\lambda_\tau|| \leq -F\lambda_n,$$
$$||\lambda_\tau|| < -F\,\lambda_n \rightarrow [\![\dot{\mathbf{u}}]\!]_\tau = \mathbf{0}, \tag{14}$$
$$||\lambda_\tau|| = -F\,\lambda_n \rightarrow \exists\,\zeta \in \mathbb{R}^+ : [\![\dot{\mathbf{u}}]\!]_\tau = \zeta\lambda_\tau.$$

With, $\lambda_\tau$, and $[\![\dot{\mathbf{u}}]\!]_\tau$ respectively, denoting the tangential contact force and displacement increment, and $F$ denoting the friction coefficient.

The the Darcy velocity in the fracture is given by

$$\mathbf{v}_F = -\frac{k_F}{\eta}\left(\nabla_\parallel p_F - \rho_{f,F}\mathbf{g}_\parallel\right), \tag{15}$$

where the permeability in the fracture, $k_F$, is related to the aperture by the cubic law by $k_F = a^2/12$. Here, $\nabla_\parallel p_F$ denotes the pressure gradient and $\boldsymbol{g}_\parallel$ the component of the gravity vector, both in the plane of the fracture. The subscript $F$ refers to quantities specific to the fracture. The cubic law gives a strongly non-linear relation between fracture aperture and fluid flow in the fracture. The mass balance equation for the fracture becomes

$$a\left(\frac{1}{B_f}\frac{\partial p_F}{\partial t} - \beta_f\frac{\partial T_F}{\partial t}\right) + \frac{\partial a}{\partial t} + \nabla_\parallel \cdot (a\mathbf{v}_F) - v^+ - v^- = aQ_{\mathrm{p,F}}, \tag{16}$$

where $v^+$ and $v^-$ are volumetric fluxes into the fracture on each side of the fracture (Figure 1b). The energy balance equation for the fracture is

$$\rho_{f,F}c_f T_F\frac{\partial a}{\partial t} + c_f a\frac{\partial(\rho_{f,F}T_F)}{\partial t} + \nabla_\parallel \cdot \left[a\left(\rho_{f,F}c_f T_F\mathbf{v}_F - \kappa_f\nabla T_F\right)\right] - w^\pm - q^\pm$$
$$= aQ_{\mathrm{T,F}}, \tag{17}$$

where $\kappa_f$ is the heat conductivity of the fluid and $w^\pm$ and $q^\pm$ are advective and conductive heat interface fluxes into to the fracture on each side.

The interface fluxes describe the flow of mass and energy between the fracture and rock matrix and are given with the following equations (Martin et al., 2005; Jaffré et al., 2011; Stefansson et al., 2021b):

$$v^\pm = -\frac{k_F}{\eta}\left(\frac{2}{a}\left(p_F - p_M^\pm\right) - \rho_{f,F}\mathbf{g}\cdot\mathbf{n}_M^\pm\right), \tag{18}$$

$$q^\pm = -\frac{2\kappa_f}{a}\left(T_F - T_M^\pm\right), \tag{19}$$

$$w^\pm = \begin{cases} v^\pm \rho_{f,M}^\pm c_f T_M^\pm & \text{if } v^\pm > 0 \\ v^\pm \rho_{f,F} c_f T_F & \text{if } v^\pm \leq 0 \end{cases}. \tag{20}$$

Where the subscript $F$ and $M$ refers to properties in the fracture and matrix respectively, and the superscript $\pm$ refers to which side of the fracture those properties are taken. On the matrix boundary, the internal boundary conditions,

$$\mathbf{u}_M^\pm = \mathbf{u}^\pm, \quad \mathbf{v}_M^\pm\cdot\mathbf{n}_M^\pm = v^\pm, \quad \mathbf{q}_M^\pm\cdot\mathbf{n}_M^\pm = q^\pm \quad \text{and} \quad \mathbf{w}_M^\pm\cdot\mathbf{n}_M^\pm = w^\pm, \tag{21}$$

ensure coupling from the variables in the matrix to the variables on the fracture wall. Here, $\mathbf{w}_M = \rho_{f,M}c_f T\mathbf{v}$ and $\mathbf{q}_M = -\kappa_e\nabla T$ respectively defines the advective and conductive heat flux in the matrix. On the fracture tips zero Neumann conditions are imposed for the mass and energy balance.

**Tensile stress and fracture propagation**

The base for our numerical study is the conceptual model for CDM described in Axelsson (1985). It assumes that reservoir fluid circulates at the bottom of a permeable hydrothermal reservoir, with the circulation extending through fractures into a less permeable layer below. The circulating fluid cools down the rock surrounding a single fracture (Figure 1a), creating tensile stresses and causing the rock to contract and the fracture to open and propagate—given that the tensile force is sufficient to overcome other forces holding the fracture closed.

Following Stefansson et al. (2021b) we consider propagation due to tensile forces, modeled by the stress intensity factor, $SI_\mathrm{I}$, given as a function of the normal component of the displacement-jump over the fracture:

$$SI_\mathrm{I} = \sqrt{\frac{2\pi}{R_d}} \left( \frac{\mu}{\kappa + 1} [\![\mathbf{u}]\!]_\mathrm{n} \right). \tag{22}$$

Where, $R_d$ is the distance between the point where the displacement jump is evaluated and the fracture tip, and the Kolosov constant for plain strain is given by

$$\kappa = \frac{B_S + 7\mu/3}{B_S + \mu/3}. \tag{23}$$

For details, see for instance Nejati et al. (2015). Furthermore, introducing a propagation criterion (Stefansson et al. (2021b), with the fracture tip propagating when $SI_\mathrm{I}$ exceeds a critical value:

$$SI_\mathrm{I} \geq SI_{Icrit}. \tag{24}$$

The critical value can be viewed as the rock toughness or the resistance of the rock to fracture.

**Notes on the numerical implementation**

The mathematical model for the thermo-poroelastic fractured medium with fracture mechanics and matrix-fracture mass and energy fluxes, is implemented in the open-source simulation tool PorePy, which is tailored for representing complex multiphysics processes in fractured porous media, see Keilegavlen et al. (2021a) for more information. The fractures are explicitly represented in the computational grid which allows for detailed modelling and provides high resolution of processes in the fracture and on the fracture-matrix interface (fracture walls). Moreover, fracture propagation is represented by extending the fracture grid, with minimal adjustments needed to the rest of the computational model.

In the computational grid, pressure and temperature are represented in both rock matrix and fracture, while the displacement is confined to the rock matrix and on the fracture walls and contact tractions are represented on the fractures (Figure 1b). The full set of degrees of freedom and their coupling structure is described in Stefansson, et al. (2021b), where implementation details including the algorithm for fracture propagation can also be found. In accordance with the conceptual model, we make the simplifying assumption that the propagation will be tensile and in the vertical direction. Therefore, the grid is aligned in the vertical direction, with the pre-existing fractures conforming to the grid, and the propagation is restricted to follow grid cell edges.
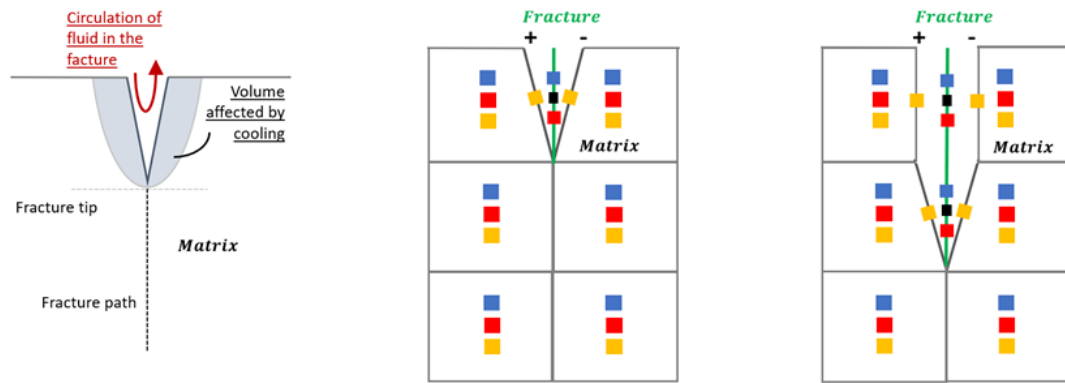
**Figure S1.** a) Conceptual model for CDM in a single open fracture, adapted from Axelsson (1985). b) Schematic of the mixed-dimensional computational grid: Pressure and temperature (blue and red) are modelled in both the rock matrix and the fracture, while the displacement (yellow) is computed in the rock matrix and on the opposing fracture walls ("+" and "-" side of the fracture). In the fracture contact traction force is shown (black) but not shown are the interface fluxes on the fracture walls, describing the flow of mass and energy between the fracture and rock matrix. c) Same schematic as b) but after the fracture has propagated one vertical grid-block downward. In the mathematical model and on the computational grid, there is no separation between the fracture and the fracture walls, still this is shown on b) and c) for visualization purposes.